

國立臺灣大學工學院應用力學研究所



碩士論文

Graduate Institute of Applied Mechanics

College of Engineering

National Taiwan University

Master Thesis

微流碟盤系統應用於血液中外吐小體之免疫親合抓取之  
研究

Centrifugal microfluidic platform enabling immunoaffinity-  
based exosome enrichment from whole blood

王啟睿

Chi-Jui Wang

指導教授：胡文聰 博士

Advisor: Andrew M. Wo, Ph.D.

中華民國 106 年 7 月

July 2017

# 國立臺灣大學碩士學位論文

## 口試委員會審定書



微流碟盤系統應用於血液中外吐小體之免疫親合  
抓取之研究

Centrifugal microfluidic platform enabling  
immunoaffinity-based exosome enrichment from  
whole blood

本論文係 王啟睿 君 (學號:R04543067) 在國立臺灣大學  
應用力學研究所完成之碩士學位論文，於民國 106 年 07 月 26  
日承下列考試委員審查通過及口試及格，特此證明

口試委員：

胡文聰

(指導教授)

沈湯龍

許聿翔

所 長

王立昇

## 致謝



轉眼間，兩年過去了，還記得當初剛踏進應力所，懷抱著滿腹的理想與對未來的憧憬，希望自己能在微流實驗室做出一些不平凡的事情。很慶幸能在這樣坐擁極大資源的環境下學習、成長。感謝實驗室的大學長姊貞伶、遠哥、韋凡，當我在實驗上遇到難以解決的問題時，總是適時的點醒我，使得我的研究之路得以繼續走下去。特別感謝助理華偉、芷琪、冠瑄在生物領域相關的協助，使得我這個工程背景的人，在遇到陌生的生物問題時，可以迎刃而解。也要感謝實驗室的碩二研究夥伴展毓、韋傑，我們一起渡過了修課的難熬，與拚畢業天天趕實驗的時光。還有碩一的學弟恆允、沐承、念文、博惟在實驗室瑣事上的協助，也都是不可或缺的存在。感謝父母、家人、女朋友、阿法、肥妞、撲嚕，總是在背後給予無限的支持，在我感到失落的時候，補充滿滿的能量，讓我得以應付每天的挑戰。最後特別的感謝我的指導老師胡文聰教授，給我不只限於知識上的協助，而更多的是心靈上的信仰，也時常給予我信心，讓我得以完成碩士論文。真的很榮幸能在這麼多實驗室夥伴的共同努力下完成碩士論文，這份兩年的回憶，將會是一輩子彌足珍貴的寶藏。

## 中文摘要



癌症轉移是目前最主要的癌症死亡原因，對於其轉移的機制至今仍待釐清。透過分析現今所認定之癌症轉移因子，盼望對於其轉移的預防能有更進一步的貢獻。近年來，外吐小體已被許多研究證實在癌症轉移中扮演著相當重要的角色，而用其當作早期癌症轉移的標的也漸趨明朗。如何精準且快速的抓取與分析高純度的外吐小體也就成為現今很重要的一個課題。本研究提出一套能運用在自動化機台的微流碟盤系統。此系統由微結構碟盤與特殊設計的微量離心管承載器所構成，碟盤可直接從全血開始進行自動化血漿分離以及外吐小體的磁珠免疫親合抓取，其免疫磁珠與血漿比例和外吐小體抓取效率則是經由 100 到 600 微升的全血進行驗證，而結果是由西方墨點法進行蛋白檢測。此外，透過與超高速離心法和高分子試劑抓取的比較，實驗結果證實，碟盤系統可從三位乳癌患者成功的分離出血漿中的外吐小體。且可從全血分離 98.3% 的紅血球以達到血漿分離。此系統透過自動化機台和免疫親合法的專一抗體結合抗原特性，減少了人為的操作實驗的誤差，同時省去了超高速離心繁瑣步驟和常用試劑的非專一抓取的問題。盼望此系統能對於未來臨床研究者提供妥善的協助。

關鍵字：微流碟盤、外吐小體、乳癌、自動化、免疫親合抓取

## Abstract



Cancer management can be better served by suitable biomarkers ranging from diagnosis and monitoring of therapeutic progress. Over the past few years, clinical relevance of exosomes as a marker during tumor progression and early disease detection has been validated. However, the enrichment of exosomes remains technically challenging, where purity, reproducibility and automation are highly desirable. In this thesis, a centrifugal microfluidic platform was presented to enrich exosomes directly from blood. The platform contains a microfluidic disk and a mechanism to collect plasma into an Eppendorf tube. A range of parameters of immunomagnetic beads to plasma ratio and system performance could be obtained from 100 to 600  $\mu$ l of human whole blood. Western blotting was used for protein quantification. Besides, the performance of exosome enrichment was compared with that from ultracentrifugation and a commercial exosome isolation kit. Results showed that the microfluidic device successfully enriches exosomes from three breast cancer patients directly from whole blood. Averaged 98.3% red blood cells from whole blood was depleted in the plasma separation process. Taken together, our microfluidic platform provides a simple-to-use and robust approach to enrich specific exosomes by recognizing the exosomal surface markers. Moreover, the automated system reduces variation in operator biases and may serve as a standard device for clinical uses.

Keywords: microfluidic, exosomes, breast cancer, automated, immunomagnetic approach

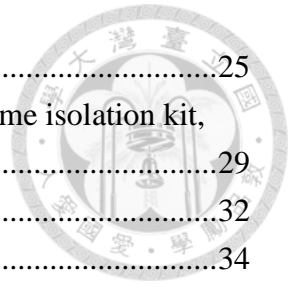


# 目錄 Table of Contents



口試委員會審定書 .....	i
致謝 .....	ii
中文摘要 .....	iii
Abstract.....	iv
目錄 Table of Contents.....	vi
圖目錄 List of figures .....	viii
表目錄 List of tables .....	ix
Chapter 1. Introduction.....	1
1.1 Clinical relevance of exosome.....	1
1.2 Technologies for exosomes enrichment.....	2
1.3 Development of exosomes enrichment via microfluidic disk system .....	6
Chapter 2. Design Feature and Methodology .....	7
2.1 Plasma separation microchannel network .....	7
2.2 Eppendorf design for exosome enrichment .....	11
2.3 System setup .....	12
Chapter 3. Materials .....	13
3.1 Materials .....	13
3.1.1 Disk and Eppendorf holder fabrication .....	13
3.1.2 Preparation of plasma .....	14
3.1.3 Preparation of conditioned medium .....	14
3.1.4 Reagents .....	15
Chapter 4. Methods .....	16
4.1 Exosomes enrichment.....	16
4.1.1 Ultra-centrifugation .....	16
4.1.2 Immunomagnetic approach .....	18
4.1.3 Total exosome isolation precipitation.....	18
4.1.4 Centrifugal microfluidic platform .....	18
4.2 Exosome detection.....	19
4.2.1 Electron microscopy .....	19
4.2.2 Immunoblotting .....	20
Chapter 5. Results and Discussion .....	21
5.1 Overview of immunoaffinity-based exosome enrichment via disk platform ....	21
5.2 Performance of plasma separation from whole blood using the disk platform.	22
5.3 Immunomagnetic exosome enrichment: disk-based versus tube-based	

approached.....	25
5.4 Comparison of performance among disk system, total exosome isolation kit, and ultracentrifugation.....	29
Chapter 6. Concluding remarks .....	32
References .....	34





## 圖目錄 List of figures



Figure 2.1 The basic principles of RBCs separation .....	9
Figure 2.2 Underlying principle of beads enrichment in Eppendorf.....	12
Figure 3.1 Fabrication of disk and Eppendorf holder.....	14
Figure 4.1 Flow chart of exosomes enrichment by ultracentrifugation.....	17
Figure 5.1 Plasma separation from whole blood on microfluidic disk.....	23
Figure 5.2 Depletion rate of disk-based and tube-based plasma separation.....	24
Figure 5.3 Scanning electron microscopy of enriched exosomes by immunomagnetic approach and ultracentrifugation.....	26
Figure 5.4 Protein quantification and western blot analysis of exosome enriched by immunomagnetic approach via pipetting platform and rotating platform ....	28
Figure 5.5 Protein concentration-ratio of volume of beads to volume of plasma .....	28
Figure 5.6 Protocol for the entire process of disk system .....	29
Figure 5.7 Overall procedures of plasma separation and exosomes enrichment.....	30
Figure 5.8 Expression of coomassie blue staining and western blot analysis in exosome enriched by ultracentrifugation, total exosome isolation kit, disk platform, and MCF7 cell lysate.....	31

## 表目錄 List of tables



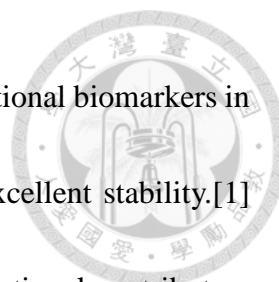
Table 1 Classification of extracellular vesicles .....	2
Table 2 The list of reagents used in this study.....	15

# Chapter 1. Introduction



## 1.1 Clinical relevance of exosome

Cancer is the second leading cause of death worldwide, and causes 8.8 million deaths in 2015.[1] The main reason that the disease is so deadly is due to metastasis of cancer cell. Metastasis is the dissemination of malignant cell from primary tumor site to colonize distant organs via the lymphatic or circulation system. Yet the mechanisms of metastasis are still unclear and the methods against to metastasis remain limited.[2] Thus, early detection of metastasis may light up tumor biology and improve cancer treatment.[3] New paragraph circulating tumor cells (CTCs) has always been regarded as (a) early detection biomarker to estimate the risk for metastatic relapse or metastatic progression, (b) real-time monitoring of therapies, and (c) mechanisms of metastasis.[4] Moreover, researchers have demonstrated that organs of future metastasis are selectively modified into pre-metastasis niches (PMNs) by tumor-secreted factors and tumor-secreted extracellular vesicles (EVs) before arrival of CTCs.[5, 6] EVs, as shown in Table 1, are critical intercellular communicators between tumor cells and stromal cells, and also are the important roles in both tumor growth and metastasis. Among the EVs subtypes, exosomes are extensively studied because of the important value of exosomes as biomarker in



clinical prognostics and diagnostics.[7] Compared with other conventional biomarkers in plasma, exosomes provide higher sensitivity and specificity, and excellent stability.[1]

Recently, exosomes are also demonstrated to be biomarkers and functional contributors to PMNs.[8] The potential clinical use of exosomes as novel biomarker may shed light on tumor predicting and preventing future metastatic development.[1, 9]

**Table 1 Classification of extracellular vesicles. [7]**

	<b>Exosomes</b>	<b>Microvesicles, ectosomes, shedding vesicles</b>	<b>Apototic bodies</b>
Origin	Endosome	Plasma membrane	Plasma membrane
Size	30-150nm	100-1000nm	1000-5000nm
Markers	Tetraspanins (CD9, CD63, CD81), Alix, TSG101	Selectin, integrin, CD40	Phosphatidylserine, histones
Contents	Proteins and nucleic acids (mRNA, miRNA and other non-coding RNAs), major histocompatibility complex molecules	Proteins and nucleic acids (mRNA, miRNA and other non-coding RNAs)	Nuclear fractions, cell organelles

## 1.2 Technologies for exosomes enrichment

The development of technology for exosomes enrichment is fundamentally difficult due to the nanoscale size of exosomes. Thus enrichment and detection of exosomes need to be extremely sensitive and specific. In recent years, growth of research in exosomes has been accelerating worldwide, and there have been prospective technologies to overcome difficulties of enrichment of exosomes. The exosome enrichment technologies



are mainly based on physical properties (e.g. size, density, and electric charge), biological properties (e.g. surface protein, surface molecules), or both.

For physical properties, ultracentrifugation (UC) is the current gold standard for exosome enrichment.[10] UC consists of multiple centrifugation steps with increasing centrifugal force to pellet cells ( $300 \times g$ ), microvesicles ( $10,000 \times g$ ), and exosomes ( $100,000 \times g$ ). Chiou et al. used sucrose gradient centrifugation to purify exosomes by ultracentrifugation in order to separate exosomes from other extracellular vesicles.[11] Another approach is size exclusion chromatography (SEC) [12, 13], which separates the EVs based on their size with several filters, and reduce the numbers of co-enriched low-density lipoprotein.[14] Still another approach is electrophoresis, Takanori et al.[15] introduced an on-chip device using the measurement platform comprising a micro-capillary electrophoresis chip and laser dark-field imaging system for exosome enrichment. And the other approach, Wang et al.[16] fabricated a microfluidic device consisting of trapping exosomes using a porous silicon micro-pillars structure.


Biological properties are mainly focused on immunoaffinity, which is the specific affinity between antibody and antigen. Immunomagnetic approach is one of the most common techniques in diagnostics. ExoCap (JSR Life Sciences) and exosome isolation kits (MACS) are the commercial products using magnetic beads to enrich exosomes by

recognizing the tetraspanin proteins CD9, CD63, or CD81 with specific antibodies.

Another approach is commercial precipitation protocol, ExoQuick (SBI) and total exosome isolation kit (Invitrogen), which contained volume-excluding polymers, generated the higher yield of concentrated exosomes, but lower purity of exosomes.[17]

Rider et al.[18] development a polyethylene glycol-based method similar with commercial precipitation, called ExtraPEG, enriched exosomes rapidly and inexpensively in higher purity using low speed centrifugation. Still other is chemical reagent approach, Brownlee et al.[19] isolated exosomes based on electrostatics with acetate, and the results were indistinguishable from exosome enrichment by ultracentrifugation.

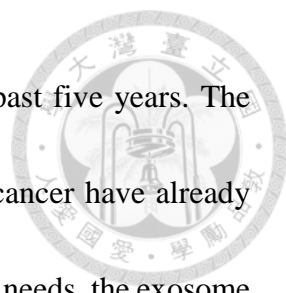
Microfluidic is making an impact in biological research. Kobayashi et al.[20] presented a microfluidic devices using the polyethylene glycol (PEG)-lipid-modified glass surface for exosomes isolation from human serum. With the glass surface, exosomes could be directly observed by atomic force microscopy. He et al.[7] developed a microfluidic approach to simplify exosomes analysis process by integrating specific immunoisolation. The phenotyping of exosomes subpopulation was also proved by multiparameter analysis of common and tumor-derived exosomal marker via their approach. In addition, Yoshioka et al.[21] described a rapid and sensitivity liquid biopsy technique called ExoScreem for profiling circulation EVs directly from whole blood



using specific antibodies. Ko et al.[22] developed a microfluidic chip using immunomagnetic beads to do both positive selection and negative selection of brain-derived exosomes, and using the smartphone camera for the convenience of exosomes detection.

Many excellent reports on specific advantages and general drawbacks of exosome associated technologies have been rising during the last decade.[23-26] Nevertheless, existing technologies, still at an early stage of development, are time-consuming, require specific equipment, reagent costly, or lack of purity. In fact, there is not any technology detailing exosome isolation from clinical setting. Each of the technologies have its own advantages and disadvantages. Briefly, exosome enrichment using immunoaffinity have the highest purity among the enrichment methods, however, the low yield of exosomal marker protein need the detection methods with high sensitivity and specificity for clinical diagnostics. Even though the ultracentrifugation has been regarded as the current gold standard. It has been indicated that ultracentrifugation co-enrich the contaminating proteins but not the selectively enrich for exosomes. Moreover, exosomes are invisible during the ultracentrifugation process. The operator-experienced operation and incorrect way of using a common protocol with different rotors may result in large variation.[27]

Because of the clinical value of exosomes, the increasing interests of exosomes in



early detection and monitoring of cancer have been proved in the past five years. The specific exosomal protein markers of pancreatic cancer and breast cancer have already been published in 2015 and 2016.[28, 29] In order to meet the clinical needs, the exosome enrichment method must reduce the variation in operator biases and fast in time. In this thesis, a centrifugal microfluidic platform enabling fully automated process including plasma separation and mixing of plasma and reagent is presented.

### **1.3 Development of exosomes enrichment via microfluidic disk system**

This work utilizes an immunomagnetic approach to enrich exosomes using a microfluidic disk system. Automated plasma separation directly from the whole blood sample and mixing of plasma and immunomagnetic beads by sequential pipetting are the main features of the disk system. Validation of the disk system was accomplished by human whole blood and commercial immunomagnetic products. Then, performance of the disk system was compared with commercial precipitation total exosome isolation kit and ultracentrifugation.



## Chapter 2. Design Feature and Methodology



### 2.1 Plasma separation microchannel network

Centrifugation is one of the important techniques applied in current biological research and clinical use. For plasma separation, red blood cells (RBCs) depleting from whole blood is easily achieved via centrifugal force. Centrifugal force is usually represented by a dimensionless parameter, relative centrifugal force (RCF) as the following expression:

$$\text{RCF} = \frac{r\omega^2}{g} \quad (1)$$

where  $r$  is the rotation radius,  $\omega$  is the angular velocity, and  $g$  is the gravity acceleration. Equation (1) shows that rotor speed and rotation radius dominate the centrifugal force.

For RBCs depletion via centrifugation, centrifugal force  $F_c$ , buoyancy force  $F_b$ , and frictional force between the cell and surroundings  $F_f$  dominate isolation effect, and the net force acts on a cell can be expressed as followed:

$$\sum F = F_c + F_b + F_f = ma \quad (2)$$

In equation (2), the equilibrium state occurs when centrifugal force is balanced by opposite drag and buoyant force, and RBCs tend to settle down with terminal velocity.

Equation (2) can be written as:

$$mr\omega^2 - mv\rho_f r\omega^2 - f \frac{\rho_c V^2}{2} A = 0 \quad (3)$$



or

$$mr\omega^2 \left(1 - \frac{\rho_f}{\rho_c}\right) - f \frac{\rho_c V^2}{2} A = 0 \quad (4)$$

where  $m$  is mass of the cell,  $r$  is the distance from the rotation center,  $\omega$  is angular velocity,  $v$  is specific volume of the cell (volume per unit mass),  $\rho_f$  is density of the surrounding medium,  $\rho_c$  is density of the cell,  $f$  is drag coefficient,  $V$  is terminal velocity, and  $A$  is the cross sectional area of cell.

In equation (4), the cell will not move relative to the medium if the density of the medium is same as that of the cell. Normally, density of RBCs is 1.06 g/ml and density of plasma is 1.026 g/ml. Therefore, the plasma separation is able to success with enough settling time and rotor speed.

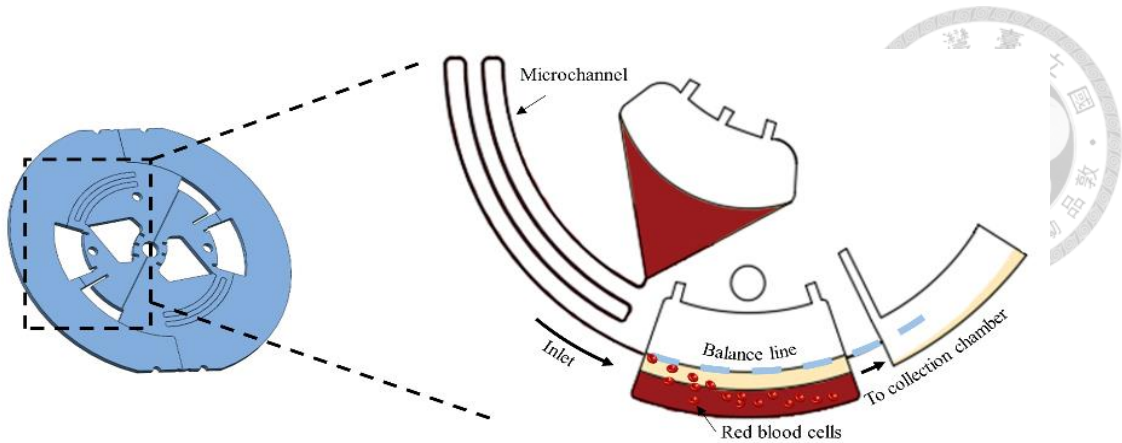


**Figure 2.1** The basic principles of RBCs separation. RBCs are sediment at the bottom of reservoir, whereas plasma run into the collection chamber. The volume under the balance line is designed by 50% of the loading whole blood sample.

As presented in Figure 2.1, the basic principles of plasma separation can be sorted into two parts, the separation design and microchannel designed. For separation design, RBCs settle to the bottom of separation reservoir due to the higher density, whereas the volume below the balance line is considering to the volume of separated RBCs from the whole blood loaded. According to American Society of Hematology, the blood is a mixture of about 55% plasma and 45% blood cells. In the design of separation, separating reservoir is able to separate 90% of the plasma from the loading whole blood sample. The flow parameter of moving RBCs along the tangential direction can be expressed as:[30]

$$q = \frac{Q}{b} = \int_{R_g}^R \sqrt{2r\omega^2} r dr \quad (5)$$

where  $q$  is the flow rate per unit width,  $\bar{r}$  is the average liquid level,  $R, R_g$  are the upstream and downstream liquid level.



In order to control the inlet flow rate, the dimension of the microchannel is designed by Equation (6):[31]

$$P_{r1} = P_{r2} - \rho r \omega^2 \Delta r + f \frac{\rho L V^2}{2D} \quad (6)$$

Where  $P_{r1}$  ,  $P_{r2}$  are the upstream and down steam fluid pressure,  $\rho$  is the fluid density,  $r$  is the distance from the rotation center,  $\omega$  is rotor angular velocity,  $\Delta r$  is the change in channel tangential distance,  $f$  is the friction factor, L is the length of the microchannel,  $V$  is the average fluid velocity, and  $D$  is the microchannel diameter.

In Equation (6), for our disk where  $P_{r1}$  and  $P_{r2}$  are inlet and outlet pressure, respectively, and are both at atmospheric pressure. Hence, the friction loss at a particular flow rate in the microchannel balances the centrifugal force. The friction factor remain constant due to the laminar flow in the microchannel. Therefore, low flow rate occurs by increases the length of the microchannel or decreases the microchannel diameter.



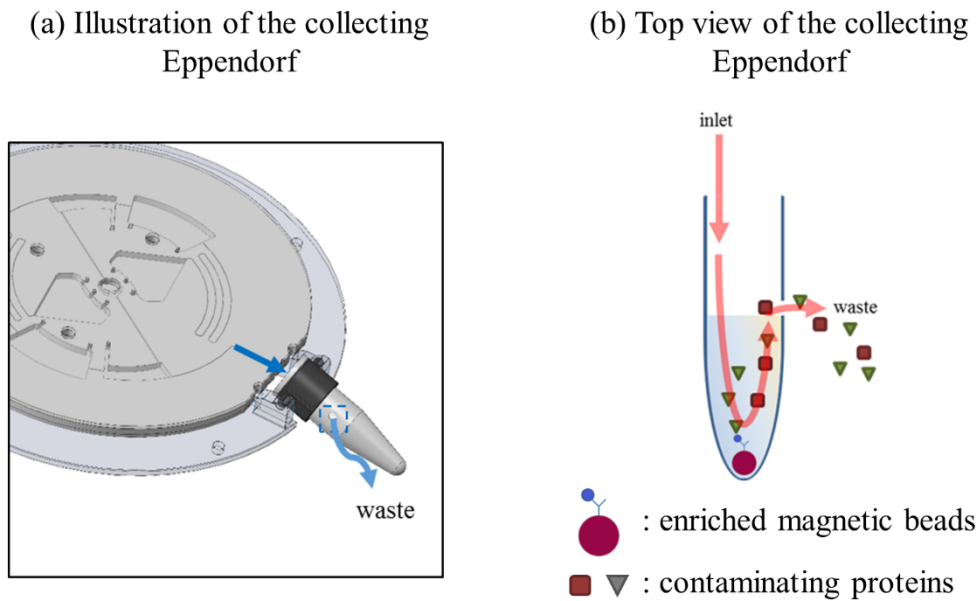
## 2.2 Eppendorf design for exosome enrichment

Figure 2.2 shows the top view of the collecting Eppendorf. When the plasma is separated from the disk and entering the collecting Eppendorf, the resultant force of centrifugal and lift force determines the liquid movement following the streamline. The sedimentation effect can be described as the Stokes' law as:

$$U_s = \frac{\rho_c - \rho_f}{18\mu} D_c^2 r_d \omega^2 \quad (7)$$

where  $\rho_c$  and  $\rho_f$  are density of the cell and the fluid,  $\mu$  is the fluid viscosity,  $D_c$  is the cell diameter,  $r_d$  is the radius of rotation, and  $\omega$  is the rotor angular velocity.

Cells are likely lost following the streamline if they are suspended and not settle down to the bottom of the Eppendorf, i.e.  $\rho_c < \rho_f$ . In other words, once cells are binded by magnetic beads, the centrifugal force will resist them from discharge hence retaining the cells in the Eppendorf.



**Figure 2.2** Underlying principle of beads enrichment in Eppendorf. (a) Beads enrichment process from disk. (b) Beads enrichment process in Eppendorf.

### 2.3 System setup

An automatic system was developed by the design of Hsu's work[32] to provide reliable and easy operation. The system is composed of an AC servo motor, a peristaltic pump, a programmable logic controller (PLC), and a touchscreen tablet computer. A high-performance servo motor produces centrifugal force and meets the needs of precision rotation speed control. A peristaltic pump was used for pipetting the sample and reagent thoroughly. PLC was used to control all the machinery components for automation achieved. Besides, touchscreen table computer aids the user in making optional decisions of the work flow.

## Chapter 3. Materials



### 3.1 Materials

#### 3.1.1 Disk and Eppendorf holder fabrication

The centrifugal microfluidic disk (Figure 3.1) was composed of three layers of polymethyl methacrylate (PMMA) sheet: a bottom plate, a structure layer, and a top layer. Except for the top layer is made from two millimeters thick PMMA, the others are made from one millimeter thick PMMA sheet. Also, the structure layer was applied with double-sided adhesive tapes (Model 4H0A, 3M Inc.). Then CO<sub>2</sub> laser engraver (Mercury II, LaserPro Inc.) was applied to cut the PMMA by reading the design drawing from computer-aided design (CAD). The narrowest microchannel is 100 $\mu$ m width to allow the blood sample to pass through. Afterwards, different layers were bonded together through the tapes with special caution in order to avoid the liquid leakage. The Eppendorf holder was composed of two main structures: disk holder and Eppendorf holder, which was designed by CAD, and fabricated by computer numerical control (CNC) machine using steel.

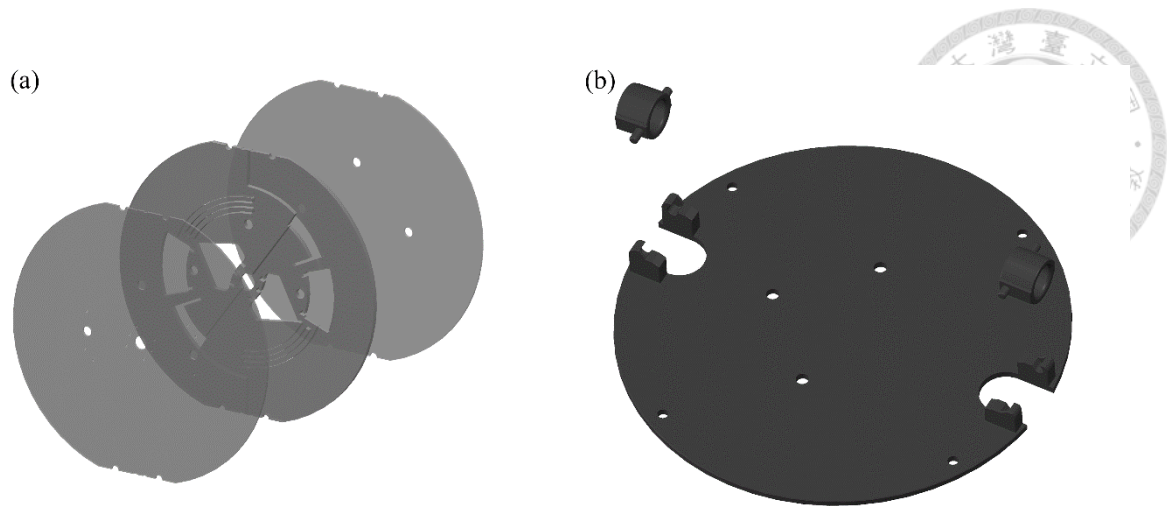


**Figure 3.1** *Fabrication of disk and Eppendorf holder. (a) Disk was composed of three layers of PMMA sheet. Double-sided adhesive tapes were applied to each PMMA sheet. (b) Eppendorf holder was composed of disk holder and Eppendorf holder.*

### **3.1.2 Preparation of plasma**

Human blood was collected into ACD tubes from healthy donors and was immediately stored at 4°C until the experiments are performed. For plasma purification, whole blood was then transferred to 15 mL tubes and centrifuged at  $\times 2000g$  for 20 minutes. Afterward, the supernatant was stored at -20°C for short term storage and -80°C for long term storage until use.

### **3.1.3 Preparation of conditioned medium**

Breast cancer cell line MCF-7 was cultured in DMEM/F12 (GIBCO, Invitrogen) supplemented with 10% fetal bovine serum (FBS), 1% penicillin-streptomycin and 1.2g/L sodium bicarbonate. Cells were grown to 80% confluency, washed three times with Dulbecco's Phosphate Buffered Saline (D-PBS) and incubated for 24 hours in serum free





medium. After the incubation, cell culture medium were collected and centrifuged for 10 minutes at 300×g to remove detached cells. Afterward, the supernatant was stored at -20 °C for short term storage and -80 °C for long term storage until use. For the preparation of the serum free medium, the DMEM was supplemented with 0.5% exosome-depleted FBS, which was obtained through 18 hours centrifugation for depleting exosomes at 100,000×g.

### 3.1.4 Reagents

Reagents used in the work are the following:

*Table 2 The list of reagents used in this study.*

Items	Vendor	Catalog No	Clone
ExoCap	JSR Life Science	EXO-COM-SP	
Total Exosome Isolation kit	ThermoFisher	4484450	
DC protein assay	Bio-Rad	5000111	
TSG101 antibody	Abcam	ab83	4A10
CD9 antibody	ThermoFisher	10626D	Ts9
IgG HRP conjugated	Rockland	18-8817-30	eB144

## Chapter 4. Methods



### 4.1 Exosomes enrichment

#### 4.1.1 Ultra-centrifugation

The ultracentrifugation protocol for exosomes enrichment is depicted in Figure 4.1. Step 1 to 3 were designed to deplete cells, dead cells, and cell debris respectively by different spinning speeds. At each of these steps, the pellet was discarded, and the supernatant was used in the subsequent step. After depleting all the non-target substances, the purified supernatant was ultracentrifuged at 100,000×g to spin down EVs, which containing exosomes. In order to eliminate contamination proteins, the EV-enriched pellet was washed in large volume of PBS and ultracentrifuged at the same high speed. Finally, the pellet of exosomes was resuspended into 50  $\mu$ L of PBS and stored at -80°C until use.

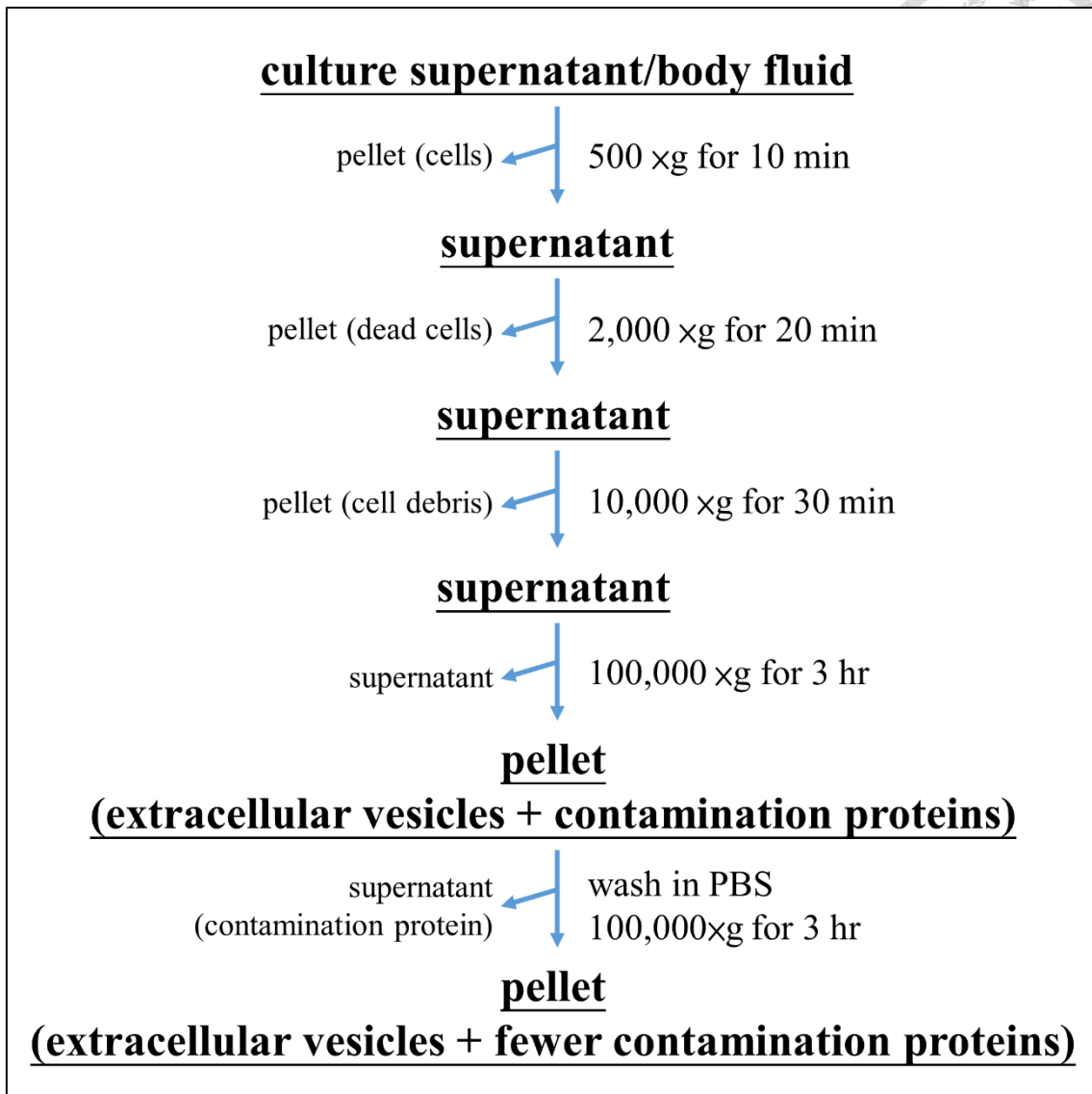


*Figure 4.1 Flow chart of exosomes enrichment by ultracentrifugation. The sample could be culture mediate or body fluid. At each centrifugation, the discarded substance (cells, dead cells, and cell debris), spinning speed, and spinning time were indicated beside the arrows.*



#### **4.1.2 Immunomagnetic approach**


The immunomagnetic approach enriched exosome by targeting exosomal surface markers. Commercial products ExoCap (MBL, Japan) and CD9 Isolation Reagent (Invitrogen, USA) were used in this study. Both reagents were pre-mixed with human plasma sample diluted (1:1) in PBS, and then incubated at room temperature for 2 hours with gentle mixing. Afterwards, spinning the tube and collecting the beads with magnetic stand for washing process. Exosomes captured by the beads was lysed and stored in  $-20^{\circ}\text{C}$  until needed.

#### **4.1.3 Total exosome isolation precipitation**

Total exosome isolation kit (TEI) was used according to the manufacturer's instructions (Invitrogen). For general case, 200  $\mu\text{L}$  of purified plasma was diluted to 300  $\mu\text{L}$  with PBS and then mixed thoroughly with 60  $\mu\text{L}$  of TEI reagent by vortexing. The sample was incubated at room temperature for 10 minutes and spun down at  $10,000\times g$  for 5 minutes. Then the pellet was resuspended in 100  $\mu\text{L}$  of PBS and stored at  $-80^{\circ}\text{C}$ .

#### **4.1.4 Centrifugal microfluidic platform**

Human whole blood was obtained from healthy volunteers and patients. 400  $\mu\text{L}$  of whole blood was pre-loaded into the microfluidic platform. Then, plasma separation




process started as the microfluidic platform rotated at 2,000 RPM for 20 minutes. After that, separated plasma was collected into the Eppendorf. For positive selection, immunomagnetic enrichment of exosomes was performed according to the manufacturer instruction of ExoCap. Briefly, 20  $\mu$ L of immunomagnetic reagent was added via a peristaltic pump into the Eppendorf containing plasma. The mixing process between immunomagnetic reagent and plasma was conducted by sequential pipetting. Afterwards, washing buffer was continuously pumped into rotating disk. Unwanted waste was depleted out of the Eppendorf due to their low density, whereas the target exosomes were enriched by immunomagnetic beads at the bottom of the Eppendorf.

## **4.2 Exosome detection**

### **4.2.1 Electron microscopy**

To examine morphology of exosomes, pellet containing exosomes enriched from cell culture medium were resuspended in DPBS and inspected by scanning electron microscopy (SEM, S-4800, Hitachi) via the following protocol. Exosomes were fixed in 2% paraformaldehyde and added on gold-coated mica, which was coated of 2 nm-5nm gold by ion sputter (E-1010, Hitachi) in order to make surface conductive. Then, the mica was air-dried and mounted on a SEM stage by carbon paste. SEM were worked under the low beam energies (3.0-5.0 kV).

## 4.2.2 Immunoblotting



Immunoblotting was performed using 4%-15% Criterion™ TGX™ Precast Gels (BioRad) with blot module (BioRad), following the protocol provided by BioRad. The sample was aliquoted to a total protein concentration of 20 µg, as determined by detergent compatible protein assay, and lysed by adding sample buffer (125 mM Tris, 2 mM EDTA·2Na, 2% SDS, and 5% β-mercaptoethanol) and heating at 95°C for 10 mins. Following electrophoresis at 200 V for 30 mins, the proteins were electrotransferred to a 0.45 µm pore size polyvinylidene difluoride (PVDF) membrane at 100 V for 30 mins. The PVDF membrane was then stained with Ponceau S (10 min at room temperature) for locating protein bands. After twice washing with PBS-T (0.5% Tween 20 in 1×PBS), the membrane was blocked with 5% w/v nonfat dry milk at room temperature with shaking for 1 hour, and then the primary antibody (1:1000) was added into blocking buffer for overnight incubation at 4°C with shaking. After incubation, the PVDF membrane was washed 5 times for 5 mins each. Then the secondary antibody diluted (1:5000) in blocking buffer was added for incubating at room temperature for 1 hour. After that, the washing process repeated 7 times and the PVDF membrane was subjected to enhanced chemiluminescence (ECL) using BioSpectrum® Imaging System (UVP).

## Chapter 5. Results and Discussion



### 5.1 Overview of immunoaffinity-based exosome enrichment via disk platform

To validate the performance of the disk system, several parameters were tested. Results will be divided into three main parts: (a) plasma separation on disk, (b) mixing efficiency of beads and plasma, and (c) system performance of disk platform. In section 5.2, parameters affecting the performance of plasma separation efficiency will be discussed first. Then, the dimension of the microchannel and the capillary valve controlled by different spin rate are presented. In section 5.3, parameters affecting the yield of exosome are discussed, followed by the specificity of immunomagnetic beads and the mixing efficiency of immunomagnetic beads and exosome. The overall performance of disk platform is presented in section 5.4, with the performance will be compared with ultracentrifugation and total exosome isolation kit, which is regarded as golden standard of exosome enrichment and a well-known commercial product, respectively.

In order to avoid the variation of plasma in human body and achieve a reliable and simple verification of the platform, plasma is collected from fresh whole blood of the

same healthy donor in each test.



## **5.2 Performance of plasma separation from whole blood using the disk platform**

The plasma separation efficiency is dominated by the operation of the capillary valve, which is controlled by the spin rate. Figure 5.1 shows the plasma separation from whole blood. After loaded 400  $\mu$ l whole blood sample into reservoir 1, as presented in Figure 5.1(a), the microfluidic disk maintained 2000 RPM spinning rate until completely separated the plasma from whole blood. When the whole process finished, plasma was collected in the Eppendorf. The result appears that the disk platform can simultaneously separate multiple blood sample in the complete process.

As presented in Figure 5.2, purity of plasma was defined by the depletion rate of red blood cells (RBCs) as:

$$\text{depletion rate} = \frac{\text{Normal ranges of RBCs counts} - \text{RBCs counts in plasma after separation}}{\text{Normal ranges of RBCs counts}} \times 100 \% \quad (8)$$

According to Leukemia & Lymphoma Society[33], the normal RBCs range is 4.7 to 6.1 million cells per microliter for men and 4.2 to 5.4 million cells per microliter for women. The depletion rate of disk-based plasma separation was compared to tube-based plasma separation, which centrifuged 2000 RPM for 15 min and collected the supernatant without disturbing the RBCs pellet. The RBCs counts was conducted using microscope





in triplicate. After the calculation, the depletion rate of the disk-based separation and the tube based separation had no statistically significant. Results suggest that the disk-based plasma separation has the same performance as the tube-based plasma separation. Higher spinning rate is needed to further increase the depletion rate of disk-based plasma separation.

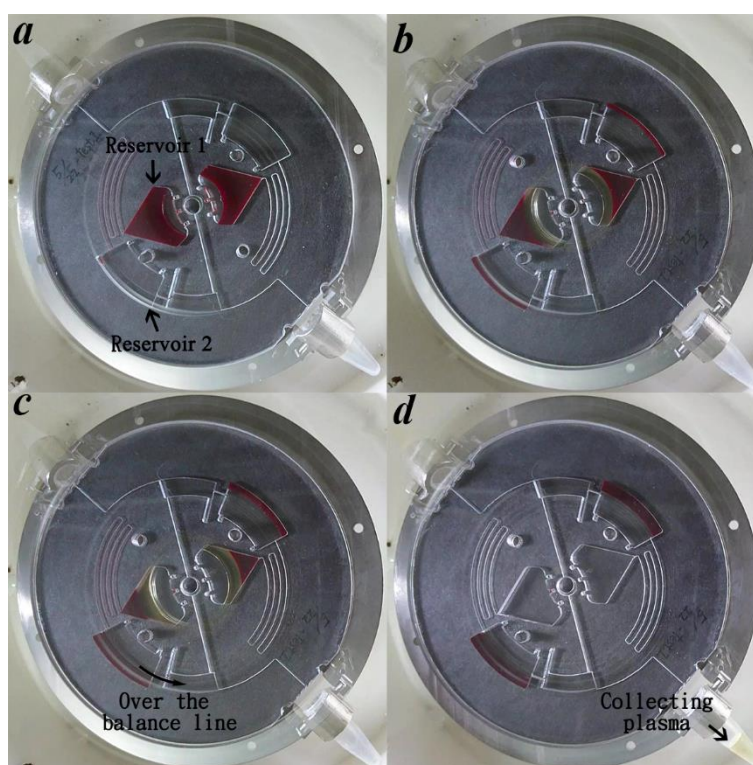
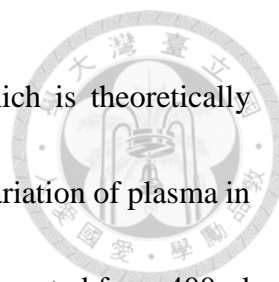


**Figure 5.1 Plasma separation from whole blood on microfluidic disk.** (a) whole blood loaded into reservoir 1. (b) plasma separated from the blood. (c) plasma is collected into Eppendorf when loading come over the limited volume of reservoir 2. (d) finish plasma collection. All of the figures are captured under 2000 RPM spinning rate with stroboscope, and it takes 15 mins to finish the whole process.



The separation efficiency is another important parameter, which is theoretically separated 200  $\mu\text{l}$  plasma from 400  $\mu\text{l}$  whole blood. Considering the variation of plasma in human body, disk-based plasma separation enables 180  $\mu\text{l}$  plasma separated from 400  $\mu\text{l}$  whole blood.

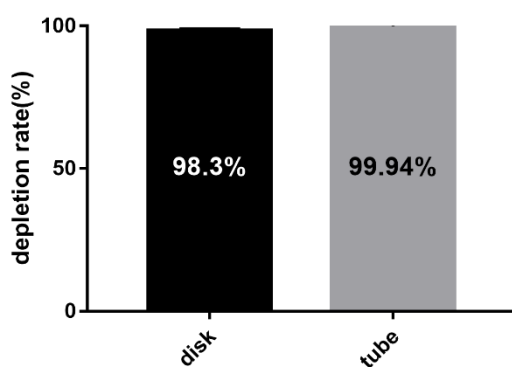


*Figure 5.2 Depletion rate of disk-based and tube-based plasma separation. 400 $\mu\text{l}$  whole blood sample were loaded, and the depletion rate of disk-based and tube-based is  $98.3 \pm 0.46\%$  and  $99.94 \pm 0.05\%$  respectively.*

### **5.3 Immunomagnetic exosome enrichment: disk-based versus tube-based approached**



The immunomagnetic approach was optimized for protein marker-specific exosome (e.g. CD9, CD63, CD81, and EpCAM). To enrich the specific exosomes, commercial product was used in the platform. Figure 5.3(a-b) showed the scanning electron microscopy (SEM) of immunomagnetic beads (2.7  $\mu\text{m}$  in diameter) incubated with PBS and plasma from healthy donor. Comparing the SEM image of the beads before and after the circulating exosome enrichment, the entire surface of bead appears densely covered with round-shape vesicles after the enrichment process. Also, in Figure 5.3(c), exosomes purified from MCF7 cell culture medium via ultracentrifugation showed the presence of exosome. Exosomes are observed in a size range from 60 nm to 100 nm in the round-shape.

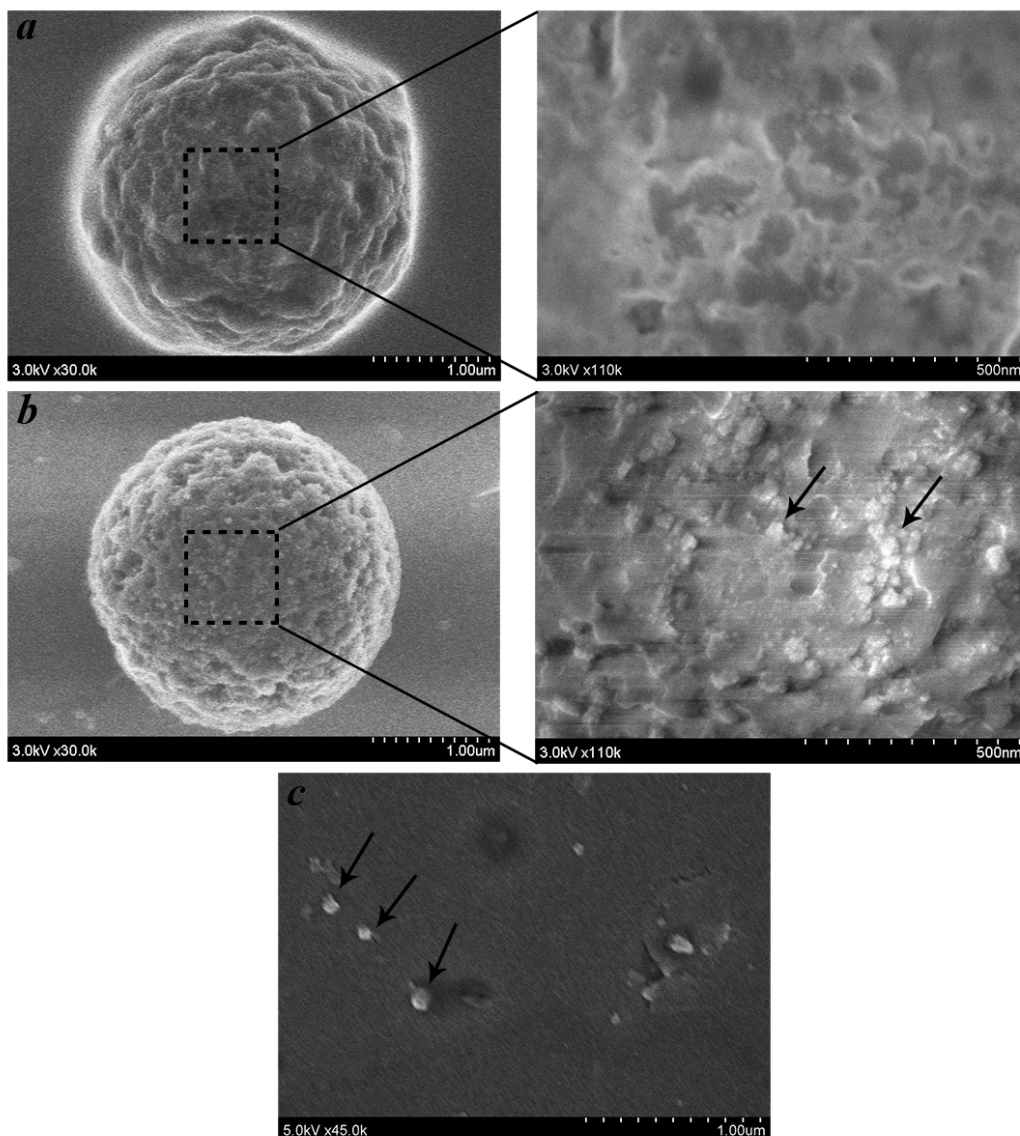
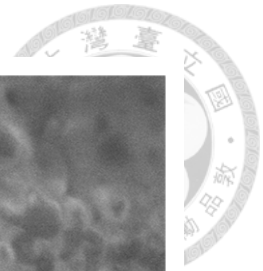


**Figure 5.3** Scanning electron microscopy of enriched exosomes by immunomagnetic approach and ultracentrifugation. (a) Scanning electron microscopy (SEM) of magnetic beads only. (left  $\times 30,000$ ; right  $\times 110,000$ ) (b) SEM of circulating exosome enriched by magnetic beads (left  $\times 30,000$ ; right  $\times 110,000$ ), arrows indicate exosome located at the bead surface. (c) SEM of solubilized exosome pellet from MCF7 cell culture media via ultracentrifugation. Arrows indicate exosomes.

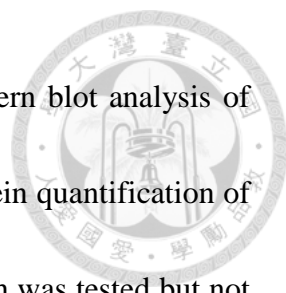
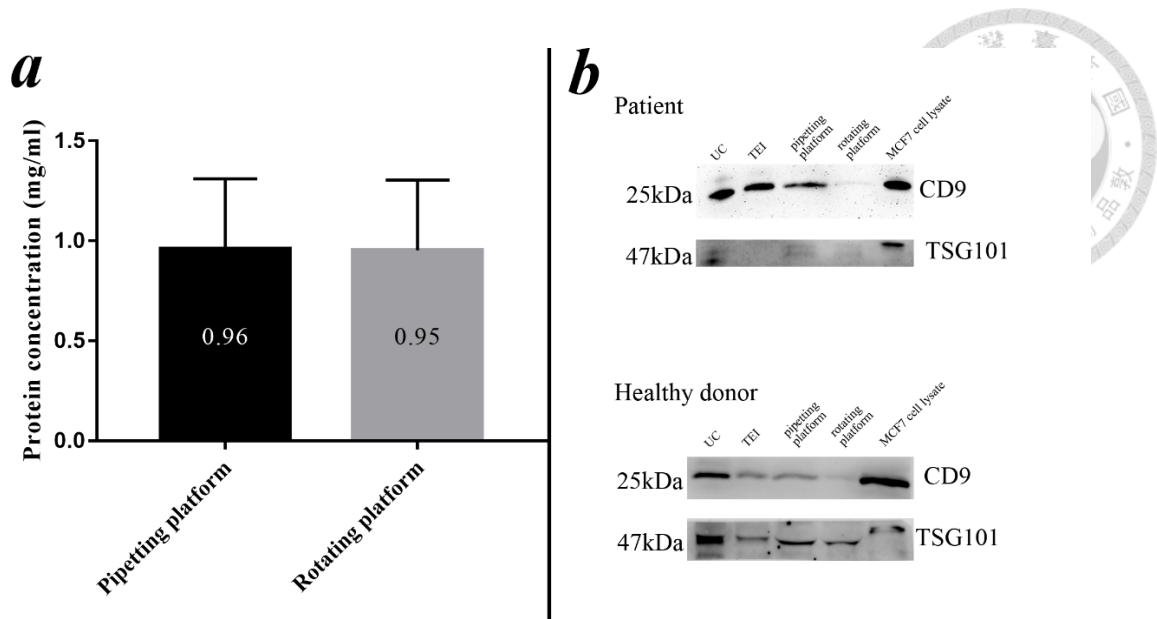
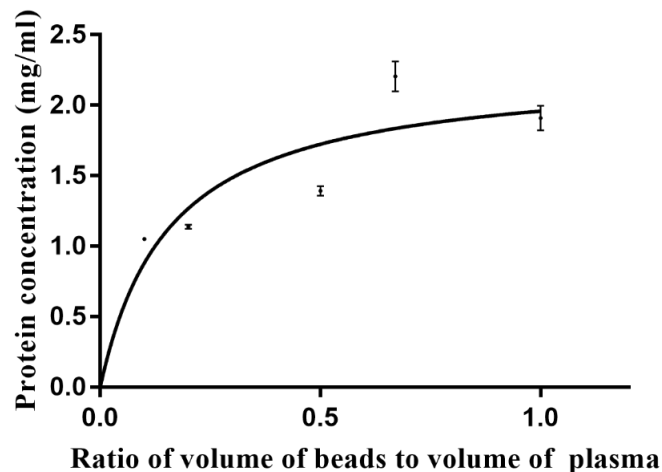


Figure 5.4 presents the protein quantification results and western blot analysis of pipetting and rotating platform via immunomagnetic approach. Protein quantification of the immunomagnetic beads only was set as a negative control, which was tested but not showed. Specifically, protein quantification of pipetting and rotating platform were 0.95 mg/ml and 0.96 mg/ml, and the negative control was 0 mg/ml. Besides, exosomal proteins CD9 and TSG101 expression were tested in western blot analysis by comparing with ultracentrifugation (UC), total exosomes isolation kit (TEI), total MCF7 cell lysate, which were the common enrichment methods and the positive control. The results appear that the pipetting platform has the higher performance than the rotating platform.

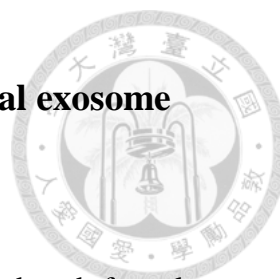
To check whether the amount of immunomagnetic beads was enough to saturate the target protein in plasma, the capacity of antibody-antigen affinity interactions between immunomagnetic beads and plasma is presented in Figure 5.5. Different ratios (from 0.1 to 1) of volume of beads to volume of plasma were tested via pipetting platform. The plateau level was reached at a ratio of 0.75. The results suggest that the optimal condition is when the ratio of beads to plasma is higher than 0.2. However, different lot of immunomagnetic beads may have different ratio.



**Figure 5.4 Protein quantification and western blot analysis of exosome enriched by immunomagnetic approach via pipetting platform and rotating platform.** (a) Protein quantification of pipetting platform and rotating platform are  $0.9607 \pm 0.2021$  and  $0.9527 \pm 0.203$  mg/ml. (b) Expression of exosomal protein marker CD9 and TSG101 shows the performance of pipetting platform versus rotating platform. UC, TEI, and MCF7 cell lysate present the common enrichment methods and positive control.



**Figure 5.5 Protein concentration-ratio of volume of beads to volume of plasma.** Different ratio of beads to plasma (1, 0.75, 0.5, 0.2, and 0.1) are mixing via the pipetting platform and the protein concentration shows the ratio above 0.2 is a suitable condition.



## 5.4 Comparison of performance among disk system, total exosome isolation kit, and ultracentrifugation

In this thesis a centrifugal microfluidic platform was introduced for plasma separation and exosome enrichment. Figure 5.6 shows the overall procedures of plasma separation and exosome enrichment via centrifugal microfluidic platform and corresponding Eppendorf holder. Figure 5.7 illustrates the entire protocol of each steps.

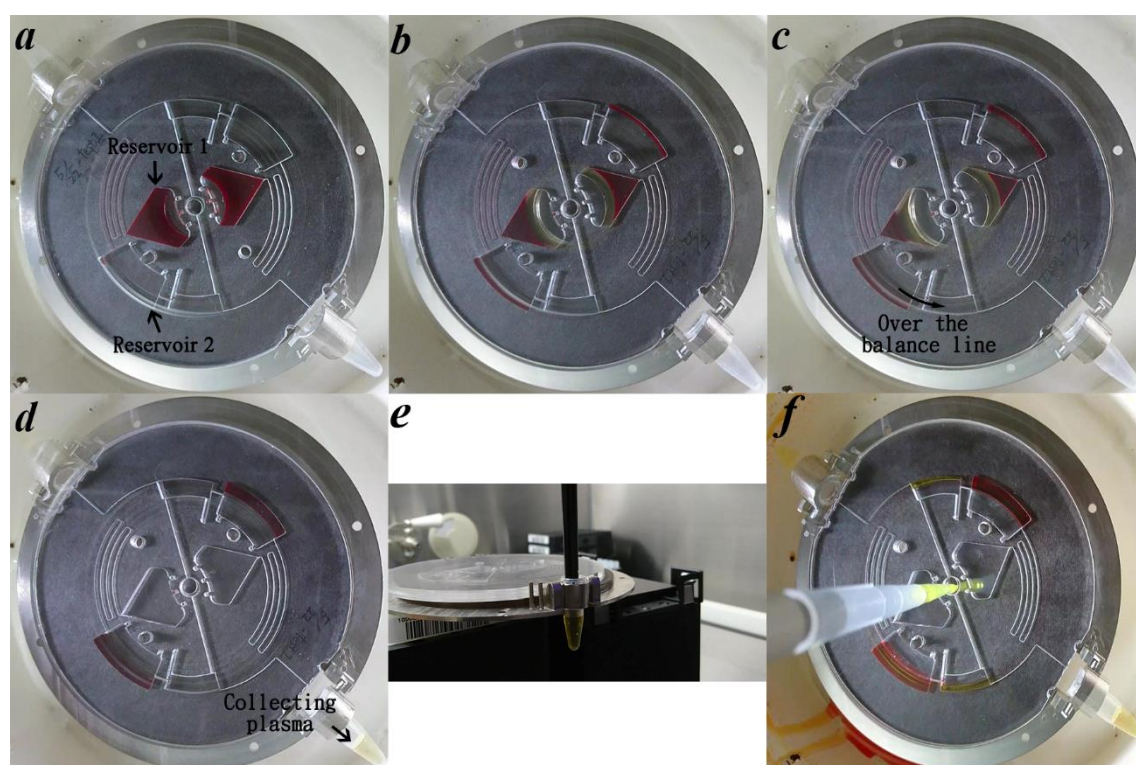


**Figure 5.6 Protocol for the entire process of disk system.** (a)-(d) Illustrate the process of plasma separation and enrichment via microfluidic disk including (a) loading whole blood sample, (b) plasma separation, and (c)-(d) plasma enrichment. (e) Illustrate the process of mixing of beads and plasma. (f) Finish all process.



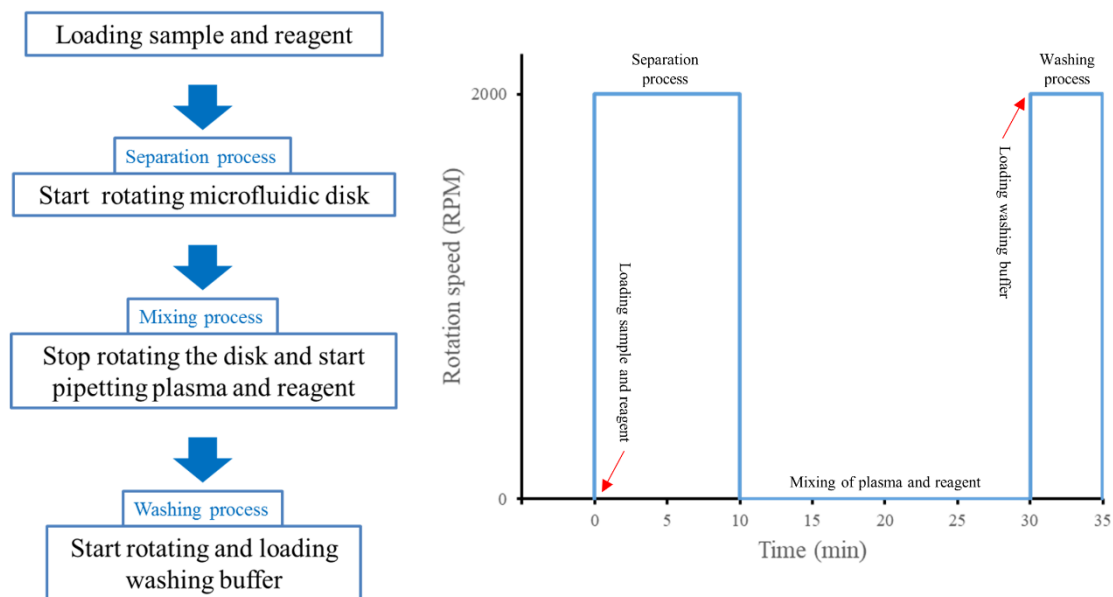


**Figure 5.7 Overall procedures of plasma separation and exosomes enrichment.**

Besides, the performance of the disk system was compared with ultracentrifugation (UC) and total exosome isolation kit (TEI). The MCF7 total cell lysate was loaded as positive control. As shown in Figure 5.8, Coomassie Brilliant Blue R (CBR) staining and exosomal tetraspanin CD9 and exosomal internal protein TSG101 were used to demonstrate the performance among different enriched method in three different patient samples. CBR staining shows the equal amount of protein (20  $\mu\text{g}$ ) was loaded into each well. Moreover, the expression of CD9 and TSG101 suggest that the performances of disk platform may be higher than UC and TEI. It seems that disk system enables to enrich exosome more precisely.



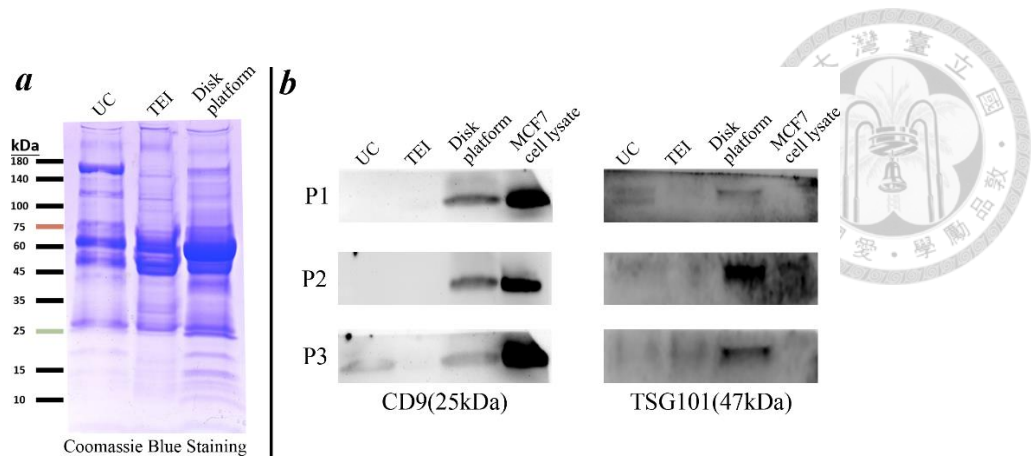


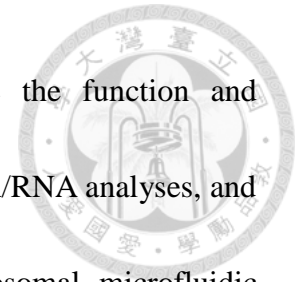
**Figure 5.8** Expression of coomassie blue staining and western blot analysis in exosome enriched by ultracentrifugation, total exosome isolation kit, disk platform, and MCF7 cell lysate. (a) Coomassie blue staining shows the total protein distribution among three enrichment methods when loading 20 $\mu$ g of protein per well. (b) Western blot analysis shows the expression of exosome protein marker CD9 and TSG101 in exosomes enriched by disk platform is higher than ultracentrifugation and total exosome isolation kit when loading 20  $\mu$ g of protein per well. P1-P2 represent three different patient samples.

## Chapter 6. Concluding remarks



This thesis presented a centrifugal microfluidic platform to enrich exosomes directly from whole blood. The process involves microchannel enabling automated sequential plasma separation and a mechanism to collect plasma into an Eppendorf tube. In order to enhance the binding of the immunomagnetic beads onto exosomal surface protein markers, pipetting approach was used in place of the traditional tube-based rotating platform. A range of parameters of immunomagnetic beads to plasma ratio and the system performance were tested using 200 to 600  $\mu\text{l}$  of human whole blood. Western blotting and total protein assay were used for protein characterization and quantification. The efficiency of plasma separation was defined by the depletion rate of red blood cells from whole blood. Besides, the performance of exosomes enrichment was compared with that from the current golden standard ultracentrifugation and the commercial product total exosome isolation kit. Results show that the microfluidic device successfully enriched exosomes from three breast cancer patients directly from whole blood. For the plasma separation efficiency, average of 98.3% red blood cells from whole blood was depleted automatically in the plasma separation process. The platform enables an easy-to-use and robust approach to enrich specific exosomes by recognizing the exosomal surface marker.

Future work should consider the following: (a) optimize the function and performance of an automatic platform, (b) enable downstream DNA/RNA analyses, and (c) establish prognostic value in patients with the present exosomal microfluidic technology.



## References



1. Lin, J., et al., Exosomes: Novel Biomarkers for Clinical Diagnosis. *The Scientific World Journal*, 2015. 2015: p. 657086.
2. Martin TA, Y.L., Sanders AJ, et al., *Cancer Invasion and Metastasis: Molecular and Cellular Perspective*. 2013: Landes Bioscience, Austin (TX).
3. Pantel, K., R.H. Brakenhoff, and B. Brandt, Detection, clinical relevance and specific biological properties of disseminating tumour cells. *Nat Rev Cancer*, 2008. 8(5): p. 329-340.
4. Alix-Panabières, C. and K. Pantel, Circulating Tumor Cells: Liquid Biopsy of Cancer. *Clinical Chemistry*, 2013. 59(1): p. 110-118.
5. Kaplan, R.N., et al., VEGFR1-positive haematopoietic bone marrow progenitors initiate the pre-metastatic niche. *Nature*, 2005. 438(7069): p. 820-827.
6. Peinado, H., et al., Pre-metastatic niches: organ-specific homes for metastases. *Nat Rev Cancer*, 2017. 17(5): p. 302-317.
7. Lötvall, J., et al., Minimal experimental requirements for definition of extracellular vesicles and their functions: a position statement from the International Society for Extracellular Vesicles. *Journal of Extracellular Vesicles*, 2014. 3: p. 10.3402/jev.v3.26913.
8. Costa-Silva, B., et al., Pancreatic cancer exosomes initiate pre-metastatic niche formation in the liver. *Nat Cell Biol*, 2015. 17(6): p. 816-826.
9. Becker, A., et al., Extracellular Vesicles in Cancer: Cell-to-Cell Mediators of Metastasis. *Cancer Cell*. 30(6): p. 836-848.
10. Witwer, K.W., et al., Standardization of sample collection, isolation and analysis methods in extracellular vesicle research. *Journal of Extracellular Vesicles*, 2013. 2(1): p. 20360.
11. Chiou, N.-T. and K.M. Ansel, Improved exosome isolation by sucrose gradient fractionation of ultracentrifuged crude exosome pellets. 2016.
12. Baranyai, T., et al., Isolation of Exosomes from Blood Plasma: Qualitative and Quantitative Comparison of Ultracentrifugation and Size Exclusion Chromatography Methods. *Plos One*, 2015. 10(12).
13. Gámez-Valero, A., et al., Size-Exclusion Chromatography-based isolation minimally alters Extracellular Vesicles' characteristics compared to precipitating agents. 2016. 6: p. 33641.
14. Sodar, B.W., et al., Low-density lipoprotein mimics blood plasma-derived exosomes and microvesicles during isolation and detection. *Sci Rep*, 2016. 6: p.

- 24316.
15. Akagi, T., et al., On-Chip Immunoelectrophoresis of Extracellular Vesicles Released from Human Breast Cancer Cells. *PLoS ONE*, 2015. 10(4): p. e0123603.
  16. Wang, Z., et al., Ciliated micropillars for the microfluidic-based isolation of nanoscale lipid vesicles. *Lab on a chip*, 2013. 13(15): p. 2879-2882.
  17. Van Deun, J., et al., The impact of disparate isolation methods for extracellular vesicles on downstream RNA profiling. *Journal of Extracellular Vesicles*, 2014. 3(1): p. 24858.
  18. Rider, M.A., S.N. Hurwitz, and D.G. Meckes Jr, ExtraPEG: A Polyethylene Glycol-Based Method for Enrichment of Extracellular Vesicles. 2016. 6: p. 23978.
  19. Brownlee, Z., et al., A novel “salting-out” procedure for the isolation of tumor-derived exosomes. *Journal of immunological methods*, 2014. 407: p. 120-126.
  20. Kobavashi, M., et al. Development of microfluidic devices with polyethylene glycol-lipid-modified adsorption surface for high- Throughput isolation of exosomes from human serum. in 17th International Conference on Miniaturized Systems for Chemistry and Life Sciences, MicroTAS 2013. 2013.
  21. Yoshioka, Y., et al., Ultra-sensitive liquid biopsy of circulating extracellular vesicles using ExoScreen. 2014. 5: p. 3591.
  22. Ko, J., et al., Smartphone-enabled optofluidic exosome diagnostic for concussion recovery. *Scientific Reports*, 2016. 6.
  23. Jørgensen, M., et al., Extracellular Vesicle (EV) Array: microarray capturing of exosomes and other extracellular vesicles for multiplexed phenotyping. *Journal of Extracellular Vesicles*, 2013. 2(1): p. 20920.
  24. Liga, A., et al., Exosome isolation: a microfluidic road-map. *Lab on a Chip*, 2015. 15(11): p. 2388-2394.
  25. Lobb, R.J., et al., Optimized exosome isolation protocol for cell culture supernatant and human plasma. *Journal of Extracellular Vesicles*, 2015. 4(1): p. 27031.
  26. Sáenz-Cuesta, M., et al., Methods for Extracellular Vesicles Isolation in a Hospital Setting. *Frontiers in Immunology*, 2015. 6: p. 50.
  27. Livshits, M.A., et al., Isolation of exosomes by differential centrifugation: Theoretical analysis of a commonly used protocol. *Scientific Reports*, 2015. 5: p. 17319.
  28. Moon, P.-G., et al., Identification of Developmental Endothelial Locus-1 on Circulating Extracellular Vesicles as a Novel Biomarker for Early Breast Cancer Detection. *Clinical Cancer Research*, 2016. 22(7): p. 1757-1766.
  29. Melo, S.A., et al., Glypican-1 identifies cancer exosomes and detects early

- pancreatic cancer. *Nature*, 2015. 523(7559): p. 177-182.
30. 徐韋凡, 負篩選卡匣式碟盤系統應用於血液中循環腫瘤細胞之分離抓取之研究. 1921.
31. Morijiri, T., et al., Microfluidic counterflow centrifugal elutriation system for sedimentation-based cell separation. *Microfluidics and Nanofluidics*, 2013. 14(6): p. 1049-1057.
32. 徐郁凱, 新型微流碟盤應用於多工處理全血中稀少細胞之分離抓取之研究, in *物理*. 2016, 臺灣大學. p. 1-39.
33. Kim, J., et al., Isolation of High-Purity Extracellular Vesicles by Extracting Proteins Using Aqueous Two-Phase System. *PLOS ONE*, 2015. 10(6): p. e0129760.